DNA Intramolecular Triplexes Containing dT → dU Substitutions: Unfolding Energetics and Ligand Binding†

Ana Maria Soto,[‡,§] Dionisios Rentzeperis,[‡,||] Ronald Shikiya,[‡,⊥] Michelle Alonso,[‡] and Luis A. Marky*[,‡,@,#]

Department of Pharmaceutical Sciences, Department of Biochemistry and Molecular Biology, and Eppley Institute for Cancer Research, University of Nebraska Medical Center, 986025 Nebraska Medical Center, Omaha, Nebraska 68198-6025

Received October 27, 2005; Revised Manuscript Received December 29, 2005

ABSTRACT: We used a combination of optical and calorimetric techniques to investigate the incorporation of deoxythymidine → deoxyuridine (dT → dU) substitutions in the duplex and third strand of the parallel intramolecular triplex d($A_7C_5T_7C_5T_7$) (ATT). UV and differential scanning calorimetry melting experiments show that the incorporation of two substitutions yielded triplexes with lower thermal stability and lower unfolding enthalpies. The enthalpies decrease with an increase in salt concentration, indirectly yielding a heat capacity effect, and the magnitude of this effect was lower for the substituted triplexes. The combined results indicate that the destabilizing effect is due to a decrease in the level of stacking interactions. Furthermore, the minor groove ligand netropsin binds to the minor groove and to the hydrophobic groove, created by the double chain of thymine methyl groups in the major groove of these triplexes. Binding of netropsin to the minor groove yielded thermodynamic profiles similar to that of a DNA duplex with a similar sequence. However, and relative to ATT, binding of netropsin to the hydrophobic groove has a decreased binding affinity and lower binding enthalpy. This shows that the presence of uridine bases disrupts the hydrophobic groove and lowers its cooperativity toward ligand binding. The overall results suggest that the stabilizing effect of methyl groups may arise from the combination of both hydrophobic and electronic effects.

It has long been recognized that control over gene expression may open the possibility of a number of therapeutic as well as biotechnological applications. In the cell, regulatory proteins modulate gene expression through specific binding to selected DNA sequences (*1*). The high affinity of proteins for their nucleic acid targets allows the formation of tight complexes that effectively inhibit and/or promote downstream interactions (*1*). To mimic the affinity and specificity of these regulatory proteins, synthetic ligands should be able to recognize nucleic acid targets differing by a single base pair. Nucleic acids and their exquisite selectivity offer a rational way of recognizing DNA or RNA sequences with high affinity and specificity (*2*). The use of nucleic acids as modulators of gene expression has been exploited through two main approaches: the antisense and antigene strategies (*3*, *4*). In the antisense strategy, an oligonucleotide (ODN)[1] binds messenger RNA and inhibits the translation of the corresponding protein (*5*). In the antigene strategy, the ODN binds to the major groove of a DNA double helix, resulting in the formation of a triple helix and inhibiting the transcription of its target gene (*6*).

The formation of triple helices is sequence specific and may interfere with transcription by competing with the binding of proteins that activate the transcription machinery (*4*, *7*). The specificity of triple helices relies on the formation of Hoogsteen hydrogen bonds between the third-strand bases and the purine bases of the duplex (*2*, *8*, *9*). Triplexes can be classified on the basis of the composition and orientation of the third strand. Antiparallel triplexes form when a purine-rich third strand is antiparallel to the purine strand of the duplex (*10*). Parallel triplexes form when a pyrimidine-rich third strand is parallel to the purine strand of the duplex (*11*), forming TAT and C^+GC base triplets (*8*). Several factors affect the stability of triple helices, including pH, salt, nucleotide sequence, base composition, base substituents, and electrostatic effects (*12*−*17*). With respect to the latter, it has been postulated that methyl groups in the C5 position of pyrimidines stabilize triplex formation (*16*, *18*−*24*). The importance of these groups is illustrated in the higher stability of triplexes containing 5-methylcytosine and thymidine over triplexes containing cytosine and uridine (*16*, *22*, *24*). Furthermore, the presence of consecutive thymidine residues

† This work was supported by Grant MCB-0315746 from the National Science Foundation. The support of a Blanche Widaman Fellowship (A.M.S.) from the University of Nebraska Medical Center is greatly appreciated.

* To whom correspondence should be addressed. Telephone: (402) 559-4628. Fax: (402) 559-9543. E-mail: lmarky@unmc.edu.

‡ Department of Pharmaceutical Sciences.

§ Present address: Department of Chemistry, The College of New Jersey, 2000 Pennington Rd., Ewing, NJ 08618.

|| Present address: Johnson&Johnson, Pharmaceutical Research & Development, LLC, 665 Stockton Dr., Exton, PA 19341.

⊥ Present address: Department of Microbiology and Immunology, Creighton University, 2500 California Plaza, Omaha, NE 68178.

@ Department of Biochemistry and Molecular Biology.

Eppley Institute for Cancer Research.

[1] Abbreviations: DSC, differential scanning calorimetry; ITC, isothermal titration calorimetry; CD, circular dichroism; UV, ultraviolet; ODN, oligodeoxynucleotide; ATT, d($A_7C_5T_7C_5T_7$); AUT, d($A_7C_5U_7C_5T_7$); ATU, d($A_7C_5T_7C_5U_7$); AUU, d($A_7C_5U_7C_5U_7$); AU_2T, d($A_7C_5T_2UTUT_2C_5T_7$); ATU_2, d($A_7C_5T_7C_5T_2UTUT_2$).

10.1021/bi052203b CCC: $33.50
Published on Web 02/08/2006

Scheme 1: (a) Sequences of Deoxyoligonucleotides and Their Designations and (b) Cartoon of the Two-Dimensional Structures of ATU_2 and AU_2T[a]

(a) Parent triplex: $^{5'}$-$A_7C_5T_7C_5T_7$-$^{3'}$ (*ATT*)

Substituted Triplexes: $^{5'}$-$A_7C_5U_7C_5T_7$-$^{3'}$ (*AUT*)

$^{5'}$-$A_7C_5T_7C_5U_7$-$^{3'}$ (*ATU*)

$^{5'}$-$A_7C_5U_7C_5U_7$-$^{3'}$ (*AUU*)

$^{5'}$-$A_7C_5T_2UTUT_2C_5T_7$-$^{3'}$ (AU_2T)

$^{5'}$-$A_7C_5T_7C_5T_2UTUT_2$-$^{3'}$ (ATU_2)

(b)

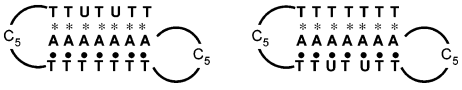

[a] Circles and asterisks represent Watson−Crick and Hoogsteen hydrogen bonds, respectively.

exhibits an additional stabilizing effect (*22*), suggesting that adjacent methyl groups interact in a favorable way, but the actual source of this stability remains unclear (*22*). One possible explanation is that in the parallel orientation, the nearby and aligned thymine methyl groups of consecutive TAT base triplets form a double chain of methyl groups in the major groove of B-DNA; this creates a hydrophobic groove that immobilizes higher levels of structural hydration. The resulting DNA triplex is more compact and stabilized with additional hydrophobic interactions (*25*). The existence of such a hydrophobic groove has been tested by investigating the binding of the minor groove ligand netropsin to a parallel intramolecular triplex with seven consecutive TAT base triplets (*25*, *26*). The binding of netropsin to this triplex, and relative to a control duplex with seven AT base pairs, indicated the presence of an additional binding site formed by both methyl groups of each TAT base triplet. The authors concluded that these methyl groups form a hydrophobic spine in the major groove because binding of netropsin to this additional site is accompanied by a high exothermic enthalpy (*25*, *26*).

To investigate the role of the methyl groups in the stability of DNA parallel triple helices, we have studied the stability of triplexes containing dT → dU substitutions. Specifically, we have replaced 14, seven, or two dT's with dU's in the $d(A_7C_5T_7C_5T_7)$ triplex of previous investigations (Scheme 1) (*25*, *26*). Our results show that this type of substitution decreases the stability of a DNA triplex, resulting in triplexes with weaker stacking interactions and lower charge density parameters. The interaction of netropsin, which is used to probe the formation of the additional hydrophobic groove, showed that this ligand recognizes two binding sites in the triplexes with two dT → dU substitutions. However, binding of netropsin to the interrupted hydrophobic spine yielded lower affinities and enthalpies. Our overall results suggest that the methyl groups have a stabilizing effect on the formation of a triplex and that this stabilization may arise from both the formation of better base triplet stacks and favorable interactions of the adjacent methyl groups.

MATERIALS AND METHODS

Materials. All oligonucleotides were synthesized by the Core Synthetic Facility of the Eppley Research Institute, HPLC-purified, and desalted by column chromatography. The concentration of the oligomer solutions was determined at 260 nm and 80 °C using the following molar extinction coefficients (ϵ) (Scheme 1): 279 mM^{-1} cm^{-1} of strands for $d(A_7C_5T_2UTUT_2C_5T_7)$, 278 mM^{-1} cm^{-1} of strands for $d(A_7C_5T_7C_5T_2UTU_2)$, 283 mM^{-1} cm^{-1} of strands for $d(A_7C_5U_7C_5T_7)$, 283 mM^{-1} cm^{-1} of strands for d(A7C5T7-C5U7), and 296 mM^{-1} cm^{-1} of strands for $d(A_7C_5U_7C_5U_7)$. These ϵ's were calculated by extrapolation of the tabulated values of the dimers and monomer bases (*27*) at 25 °C to high temperatures, as reported previously (*28*). Buffer solutions consisted of 10 mM sodium phosphate buffer (pH 7.0) adjusted to appropriate sodium concentrations with NaCl. Netropsin was purchased from Sigma and used without further purification, and its solution concentration was determined at 296 nm using an ϵ value of 21 500 M^{-1} cm^{-1} (*29*).

Circular Dichroism (CD). Evaluation of the conformation of each triplex was obtained by simple inspection of their CD spectrum. These spectra were obtained on a Jasco J-710 spectropolarimeter, using a 10 mm quartz cuvette. All spectra were collected at room temperature, between 200 and 400 nm, using a wavelength step of 0.5 nm, and represent the average of at least two scans.

Temperature-Dependent UV Spectroscopy (UV Melts). Absorbance versus temperature profiles (melting curves) for each molecule were measured at 260 nm with a thermoelectrically controlled Aviv 14-DS spectrophotometer, as a function of strand and salt concentration, using a heating rate of ~0.6 °C/min. These melting curves allow us to measure transition temperatures (T_M) which are the midpoint temperatures of their order−disorder transitions, van't Hoff enthalpies (ΔH_{vH}) using two-state transition approximations as reported previously (*30*), and the differential thermodynamic binding of counterions (Δn_{Na^+}) between each triplex and its random coil state.

Differential Scanning Calorimetry (DSC). Excess heat capacities as a function of temperature melts for the helix coil transition of each triplex were measured with a Microcal Inc. (Northampton, MA) MC-2 differential scanning calorimeter. Two cells, the sample cell containing 1.6 mL of oligomer solution and the reference cell filled with the same volume of buffer solution, were heated from 10 to 100 °C at a heating rate of 0.75 °C/min. Analysis of the resulting thermograms, using procedures described previously (*30*), yielded standard thermodynamic profiles (ΔH_{cal}, ΔS_{cal}, and $\Delta G_{cal}°$) and model-dependent van't Hoff enthalpies (ΔH_{vH}) for the unfolding of each triplex.

Isothermal Titration Calorimetry (ITC). Binding heats for the interaction of netropsin with each triplex were measured directly by isothermal titration calorimety using the Omega calorimeter from Microcal Inc. The instrument was calibrated electrically by means of known standard pulses. A 25 μM triplex solution, placed in the reaction cell, was titrated with a 0.600 mM netropsin solution using a 250 μL syringe; both solutions were in 10 mM sodium phosphate buffer and 1.1 M NaCl (pH 7). A full titration corresponds to multiple injections of 5 μL of the netropsin solution until 130% saturation of the triplex is reached. Rotation of the syringe paddle at 400 rpm ensured complete mixing of the reactants. The heat of mixing for each injection is calculated from the resulting peak area by correction for the ligand dilution heat. The resulting calorimetric titration corresponds to the average

of at least two titrations. Analysis of the calorimetric binding isotherm, normalized heats as a function of the added titrant, using Origin (version 2.9), allows us to obtain binding enthalpies (ΔH_b), binding affinities (K_b), and the stoichiometry of the complexes (n) by fitting the binding isotherm with one or two sets of binding profiles (ΔH_b, K_b, and n).

CD Titrations. The stoichiometries of the netropsin−triplex complexes were primarily determined from ITC experiments. Alternatively, these stoichiometries were determined in CD titrations. CD titrations at 5 °C were conducted in an AVIV (Lakewood, NJ) model 202-SF circular dichroism spectrometer, using a 10 mm quartz cuvette. A 5 μM triplex solution is titrated with a 330 μM netropsin solution, using injections of 5 μL until 130% saturation is reached. The CD spectrum was recorded after each addition of the ligand. The resulting plots of ellipticity at 310 nm versus the netropsin/triplex molar concentration ratio yielded stoichiometric binding curves from which distinctive linear dependences are obtained. The break points of the resulting lines correspond to netropsin/triplex concentration ratios that yielded complex stoichiometry.

RESULTS

Effect of the Incorporation of Deoxyuridines on Triplex Stability. To establish the relative stability of the triplexes containing dT → dU substitutions, initial UV melts of intramolecular triplexes with seven dU's in the Crick strand (AUT) or Hoogsteen strand (ATU) or with a total of 14 dU's in these strands (AUU) were conducted in 0.5−1.1 M NaCl. Analysis of their melting curves yielded T_M's of 46.2 (ATU), 42.7 (AUT), and 37.5 °C (AUU), in 1.1 M NaCl, which were lower than the T_M of 52.4 °C reported for the parent triplex (ATT) at this salt concentration (*25*). This indicates that the presence of dU's has a large destabilizing effect, which will not allow these triplexes to form 100% at the lower salt concentrations used in the previous studies of ATT, particularly, in netropsin binding studies. We have then focused our thermodynamic investigation on the triplexes with only two substitutions, AU_2T and ATU_2.

UV Melting Curves. UV melting experiments were used to characterize the helix → coil transition of each triplex. Typical UV melts of AU_2T and ATU_2 are shown in Figure 1. Above 10 °C, both triplexes melt in monophasic transitions, following the characteristic sigmoidal behavior for the unfolding of a nucleic acid helix. UV melts at different total strand concentrations were conducted to determine both the T_M dependence on strand concentration and model-dependent van't Hoff enthalpies, from the analysis of the shape of the resulting curves. The T_M dependence on strand concentration for each triplex is shown in Figure 1b. Over a 70-fold concentration range, the T_M's of AU_2T and ATU_2 are independent of strand concentration, confirming the formation of intramolecular triplexes. We used the resulting melting curves and the equation (*30*) $\Delta H_{vH} = 4RT_M^2(\partial\alpha/\partial T)_{T=T_M}$ to calculate average ΔH_{vH}'s of −45 (AU_2T) and −47 kcal/mol (ATU_2) for the formation of these triplexes.

Triplex Conformation. The CD spectra of AU_2T and ATU_2 are shown in Figure 2a. Both triplexes exhibit CD spectra characteristic of right-handed helices in the "B" conformation, with similar magnitudes of the positive (∼278 nm) and negative (∼245 nm) bands. In addition, these triplexes present a negative band centered at 210 nm, which is characteristic of triple helices (*14*, *15*).

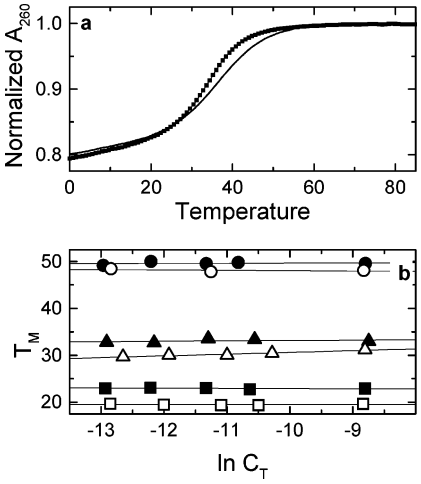

FIGURE 1: (a) UV melts of ATU_2 (—) and AU_2T (■) in 10 mM sodium phosphate buffer and 1100 mM NaCl (pH 7). (b) Dependence of T_M on the strand concentration of ATU_2 (filled symbols) and AU_2T (empty symbols) in 10 mM sodium phosphate (pH 7.0) at sodium concentrations of 16 (■), 116 (▲), and 1116 mM (●).

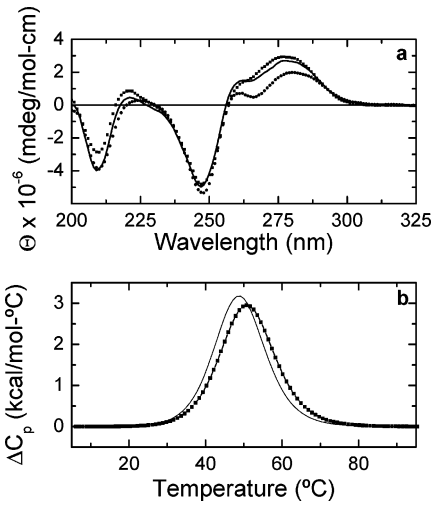

FIGURE 2: (a) CD spectra of the parent triplex ATT (●), AU_2T (■), and ATU_2 (—) in 10 mM sodium phosphate buffer and 1.1 M NaCl (pH 7.0). (b) DSC scans of AU_2T (—) and ATU_2 (■) in 10 mM sodium phosphate buffer and 1.1 M NaCl (pH 7.0).

Calorimetric Unfolding of Triplexes. Typical DSC melting curves for the unfolding of AU_2T and ATU_2 are shown in Figure 2b, and the thermodynamic profiles for the folding of each triplex at 5 °C are summarized in Table 1. The ΔH_{cal} and ΔS_{cal} parameters were measured directly using the equations $\Delta H_{cal} = \int \Delta C_p{}^a \, dT$ and $\Delta S_{cal} = \int (\Delta C_p{}^a/T) \, dT$, where $\Delta C_p{}^a$ is the anomalous heat capacity during the unfolding process. The free energy at 5 °C ($\Delta G_{278}°$) is obtained from the Gibbs equation $\Delta G_{278}° = \Delta H_{cal} - T\Delta S_{cal}$. Inspection of Table 1 indicates that the folding of each triplex at 5 °C is accompanied by favorable free energy terms resulting from the characteristic compensation of a favorable enthalpy and unfavorable entropy terms. In general, these favorable enthalpy terms correspond mainly to contributions from base pairing, base stacking, and the immobilization of water around charges (electrostricted hydration), while the unfavorable entropy terms arise from contributions of the unfavorable ordering of strands, counterion condensation, and

Table 1: Thermodynamic Profiles for the Formation of Triplexes at 5 °C

[Na^+] (mM)	T_M (°C)	$\Delta G_{cal}°$ (kcal/mol)	ΔH_{cal} (kcal/mol)	$T\Delta S_{cal}$ (kcal/mol)	ΔC_p (kcal mol^{-1} $°C^{-1}$)	ΔH_{vH} (kcal/mol)	Δn_{Na^+} [(mol of triplex)$^{-1}$]
				AU_2T			
16	19.6	−3.3	−65.5	−62.2	0.27	−50	−1.85
116	31.2	−5.3	−61.4	−56.1		−47	−2.18
1116	48.1	−7.8	−57.8	−50.0		−47	−2.52
				ATU_2			
16	22.9	−4.1	−67.0	−63.0	0.31	−42	−2.73
116	33.0	−5.8	−62.9	−57.1		−42	−2.39
1116	49.6	−8.0	−58.1	−50.1		−43	−1.99
				ATT[a]			
16	24.5	−6	−92.0	−86.0	0.70	−57	−3.38
107	33.3	−7.5	−80.9	−73.8		−50	−3.19
1100	52.4	−10.5	−71.9	−61.4		−59	−2.81

[a] Thermodynamic profiles for this triplex were taken from refs *25* and *26*. Experiments were conducted in 10 mM sodium phosphate buffer (pH 7.0), adjusted to the desired sodium concentration with NaCl. The experimental uncertainties are given here: ±0.5 °C for T_M, ±3% for ΔH_{cal}, ±5% for $\Delta G°$, ±5% for $T\Delta S$, and ±10% for ΔH_{vH}.

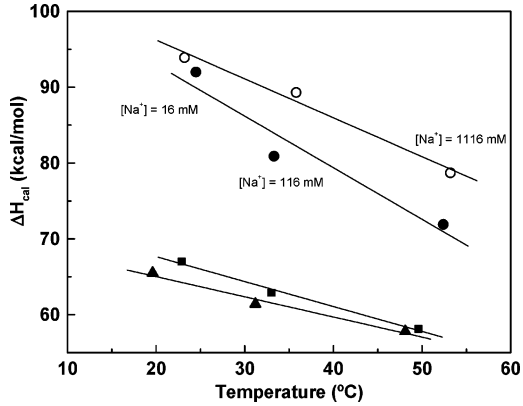

FIGURE 3: Dependence of the unfolding enthalpy on salt concentration: ATT (● and ○), ATU_2 (■), and AU_2T (▲). All values were determined in DSC experiments using a 10 mM sodium phosphate buffer adjusted to the appropriate salt concentration as roughly indicated in the figure. The filled circle values are from ref *26*, while the empty circles values correspond to additional determinations from this work.

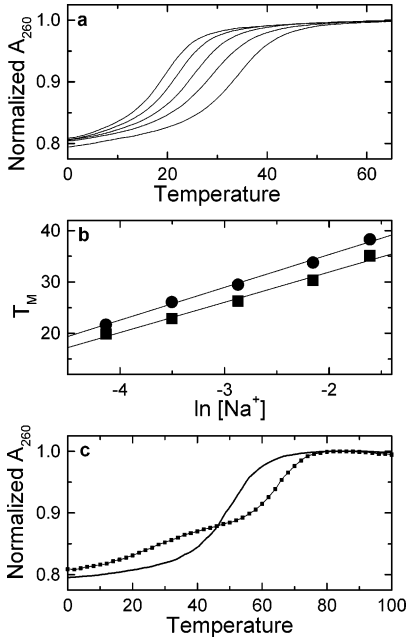

FIGURE 4: (a) UV melts of AU_2T as a function of sodium concentration, from 16 to 200 mM. (b) Dependence of T_M on sodium concentration for AU_2T (■) and ATU_2 (●). (c) UV melts of ATU_2 in 10 mM sodium phosphate and 1.1 M NaCl (pH 7.0) in the presence (■) or absence (—) of 2 equivalents of netropsin.

the ordering of water molecules. Closer inspection of Table 1 indicates that the incorporation of dT → dU substitutions, relative to ATT and in this range of salt concentration, decreases both the stability of AU_2T (average $\Delta\Delta G°$ of 2.5 kcal/mol) and ATU_2 ($\Delta\Delta G°$ of 2 kcal/mol) and their exothermic folding enthalpies, suggesting that the presence of dU bases yields a decrease in the level of stacking interactions. In addition, van't Hoff enthalpies (Table 1) were calculated from the shape of the calorimetric curves, and the large difference between the van't Hoff and calorimetric enthalpies indicates that these triplexes unfold in non-two-state transitions. We did not find heat capacity effects between the initial and final states in the DSC melting curves; i.e., $\Delta C_p = 0$. However, small heat capacity effects may be present, but the sensitivity of the MC-2 calorimeter does not allow their direct determination, as these are within the experimental noise of these curves (~100 cal mol^{-1} $°C^{-1}$). On the other hand, Figure 3 shows that the endothermic unfolding enthalpies of AU_2T and ATU_2 decrease linearly as the sodium concentration increases, with correlation coefficients of >0.96 in the linear fits. This shows indirectly the presence of heat capacity effects. The slope of the ΔH_{cal} versus T_M plots yielded apparent heat capacities of −0.27 (AU_2T) and −0.31 kcal mol^{-1} $°C^{-1}$ (ATU_2). These heat capacity values are smaller than the ΔC_p of −0.70 kcal mol^{-1} $°C^{-1}$ of ATT (*26*) or the −0.51 kcal mol^{-1} $°C^{-1}$ value obtained in similar experiments with this triplex (Figure 3). Thus, the incorporation of two dU bases results in a reduction of the heat capacity effect, which is consistent with weakened hydrophobic contributions from the disrupted double chain of dT methyl groups in the helical state of these triplexes.

Thermodynamic Release of Counterions. The UV melting curves as a function of sodium concentration of AU_2T are shown in Figure 4a, and the T_M dependences on salt concentration of ATU_2 and AU_2T are shown in Figure 4b. As the concentration of sodium increases, the T_M increases, consistent with the stabilizing effect of cations on nucleic acid helices. The thermodynamic release of counterions (Δn_{Na^+}) is determined from the standard thermodynamic relationship $\Delta n_{Na^+} = \partial \ln K / \partial \ln [Na^+]$, where K is the reaction

constant for the helix → coil transition of each DNA molecule. In this equation, a similar type of sodium binding to each state of DNA is assumed; therefore, Δn_{Na^+} corresponds to the differential binding of counterions between the helical and random coil states of DNA. Application of the chain rule yields the relationship $\Delta n_{Na^+} = (\partial \ln K/\partial T_M)(\partial T_M/\partial \ln[Na^+]) = 1.11(\Delta H_{cal}/RT_M^2)(\partial T_M/\partial \ln[Na^+])$. The first term in parentheses results from the van't Hoff relationship, which is obtained directly in DSC experiments without any assumption on the transition cooperativity, and R is the universal gas constant. The second term in parentheses corresponds to the slope of T_M versus $\ln[Na^+]$ plots, and it is obtained experimentally from UV melting curves at several salt concentrations; 1.11 is a proportionality constant for converting ionic activities into concentrations. The resulting Δn_{Na^+} values are summarized in Table 1 for the formation of triplexes; i.e., the negative values correspond to an uptake of counterions. Table 1 shows that at each salt concentration, ATU_2 and AU_2T exhibit a lower release of counterions than ATT. This suggests that the presence of dU bases in the stem of these triplexes decreases their charge density parameter if one assumes similar coil states among these three oligonucleotides at high temperatures. The actual magnitude of Δn_{Na^+} depends on both the location of the substitutions and the salt concentration used, and the overall effect is more pronounced when the dT → dU substitutions are placed in the pyrimidine strand of the duplex. Furthermore, as the salt concentration is increased, the Δn_{Na^+} values decreased for ATU_2 and ATT and increased for AU_2T.

Effect of Netropsin on Triplex Stability. The effect of netropsin on triplex stability is first analyzed from UV melting experiments. The UV melts of free ATU_2 and 2:1 netropsin−ATU_2 complexes are shown in Figure 4c. In the presence of netropsin, ATU_2 and AU_2T melted in biphasic transitions, disrupting the cooperative melting behavior of the triplex → coil transition. This suggests that netropsin binding stabilizes the duplex → coil transition but destabilizes the triplex → duplex transition. Analysis of the resulting UV melts indicates that these triplexes can still form below 8 °C, allowing us to conduct ITC and CD titrations below 8 °C.

Isothermal Titration Calorimetry. A representative ITC titration for the interaction of netropsin with ATU_2, and the corresponding binding isotherm, is shown in Figure 5. Each injection yielded exothermic heats all the way to saturation of the oligonucleotide; however, the overall shape is complex. The initial injections are less exothermic, due to an endothermic contribution for the removal of water from the minor groove (*31*), and the heat of the following injections exhibits an increased exothermicity due to the presence of two types of binding sites with different binding enthalpies; then, the injection heats are gradually reduced until saturation is approached at three bound netropsin molecules per triplex.

Thermodynamic profiles for the interaction of netropsin with ATU_2 and AU_2T, obtained from fitting the experimental binding isotherms, are summarized in Table 2. The interactions of netropsin with these triplexes exhibit exothermic enthalpies, binding affinities of 10^4-10^7, and multiple-site binding stoichiometries. Comparison with the thermodynamic profiles of the netropsin−ATT system (in the first two rows of Table 2) indicates that the presence of dU's increases the affinity of netropsin for the first site (minor groove) but

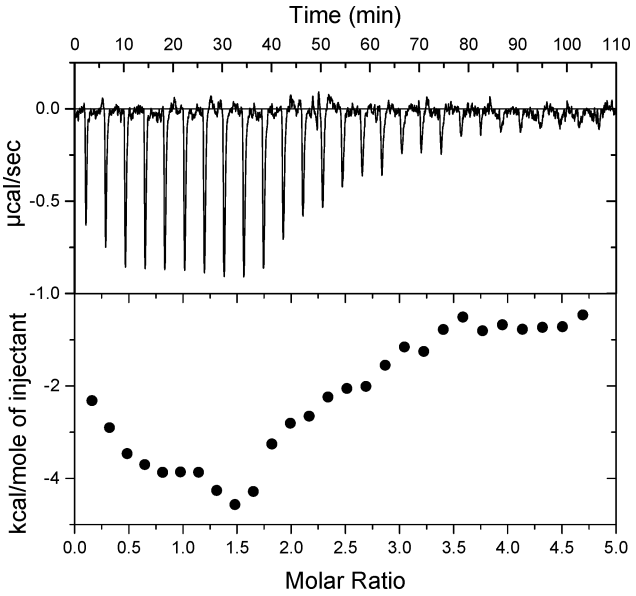

FIGURE 5: ITC titration of AU_2T with netropsin in 10 mM sodium phosphate buffer (pH 7) and 1.1 M NaCl.

Table 2: Thermodynamic Profiles for the Binding of Netropsin to Triplexes[a]

site	n	ΔH_b (kcal/mol)	K_b (M^{-1})	$\Delta G_b°$ (kcal/mol)	$T\Delta S_b$ (kcal/mol)
		ATT[b]			
minor groove	1	−2.3	4.4×10^5	−7.2	4.9
additional groove	1	−12.4	1.8×10^5	−6.7	−5.7
		ATU_2			
minor groove	1	−4.0	1.5×10^7	−9.8	5.8
additional groove	2	−8.3	4.2×10^4	−5.9	−2.4
		AU_2T			
minor groove	1	−4.4	1.8×10^7	−9.2	4.8
additional groove	2	−8.2	4.2×10^4	−5.9	−2.3
		Duplex[b]			
minor groove	1	−5.8	1.8×10^7	−9.3	3.5

[a] Experiments were conducted at 6 °C, in 10 mM sodium phosphate buffer (pH 7) and 1100 mM NaCl. Experimental uncertainties are given here: ±10% for n, ±3% for ΔH_b, ±50% for K_b, ±5% for $\Delta G_b°$, and ±5% for $T\Delta S_b$. [b] These binding profiles were taken from ref *25*.

decreases the affinity for the second binding site. The binding heats follow a trend similar to that of the binding affinities; the ΔH_b for the minor groove is larger, by ∼1.9 kcal/mol, while the ΔH_b for the second site is smaller, by ∼4.1 kcal/mol. The main observation is that the presence of two dU bases in ATU_2 and AU_2T results in the binding of two netropsin molecules to the second site. This indicates that the presence of dU's changes the overall size of the second binding site, yielding the association of an additional netropsin molecule.

CD Titrations. CD titration experiments were performed to confirm the stoichiometries of each complex. Netropsin is not an asymmetric molecule and as such, it does not have a CD spectrum on its own. However, upon binding to the minor groove of B-DNA, it exhibits an induced Cotton effect with a band centered at ∼310 nm (*26*). The CD spectra characterizing the interaction of netropsin with AU_2T are shown in Figure 6a, and the CD titrations for the interaction of netropsin with ATU_2 and AU_2T are shown in Figure 6b. Binding of the first netropsin results in the induction of a positive band at 310 nm, which increases in magnitude as

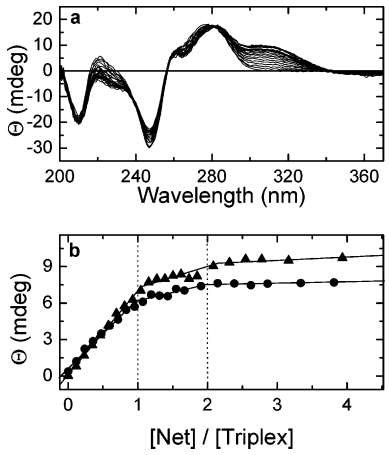

FIGURE 6: (a) CD spectra of AU_2T with increasing netropsin concentrations. (b) CD titrations of AU_2T (▲) and ATU_2 (●) with netropsin at a wavelength of 310 nm. The experimental error in the ellipticity values corresponds to the size of the symbols (±0.3 mdeg).

the ligand concentration increases, while binding of the second netropsin is accompanied by a much smaller induced CD signal. The resulting CD binding isotherms yielded three linear dependences (Figure 6b). In each case, the break points of the lines occur at netropsin:triplex molar ratios of 1 and 2. These stoichiometries confirm the multiple sites observed in ITC, although the stoichiometries from ITC are greater (three ligands per triplex). This apparent discrepancy may be reflecting the weaker binding affinity of the second site, which yielded smaller ellipticity changes. Alternatively, the CD properties of the complex with three bound ligands may differ slightly from those of the complex with two ligands.

DISCUSSION

Triplex Design. All molecules were designed to fold into intramolecular triplexes for the simple reason that these triplexes are more stable than their bimolecular or trimolecular counterparts, due to a smaller entropy penalty, allowing us to study them at lower ionic strengths. This is particularly important for this work because it was anticipated that the presence of deoxyuridines would yield a destabilizing effect on triplex formation. As shown in Figure 1, the T_M's of ATU_2 and AU_2T are independent of strand concentration, confirming the formation of intramolecular triplexes. However, these sequences could potentially form an intramolecular duplex with a dangling end or a hairpin with a large loop of 17 residues. These alternative structures are unlikely to form because the reported T_M's and enthalpies are larger than expected for the melting of seven consecutive dA·dT Watson−Crick base pairs. Thus, the observed enthalpy values of ∼62 kcal/mol suggest additional base pairing and base stacking interactions, consistent with the formation of an intramolecular triplex.

Our initial studies included four triplexes, in which the triplex used in the studies of Rentzeperis and Marky (*25*) was modified by the incorporation of dU bases. The initial UV melting curves indicate that the presence of deoxyuridines destabilizes triplex formation. This destabilization increases as the number of deoxyuridines increases, with ΔT_M's of 14.9, 9.7, and 2.8−4.3 °C for the incorporation of 14, seven, and two dU's, respectively.

Binding of netropsin destabilizes triplex formation to the extent that the formation of ATT could be guaranteed only below 14 °C in 1.1 M NaCl (*25*, *26*). The destabilizations of 9.7 (ATU) and 14.9 °C (AUU) will eliminate triplex formation in the presence of netropsin. Therefore, we focused our thermodynamic characterization on ATU_2 and AU_2T, which should form complete triplexes in the presence of netropsin up to 8 °C. The UV melting profiles of Figure 4c, which indicates that the triplex → duplex transition (with a dangling tail) has a T_M of ∼24 °C, under solution conditions of the CD and ITC titrations, confirming the complete formation of intramolecular triplexes at <8 °C.

UV melts indicate that ATU_2 is more stable than AU_2T, which may be explained by the different strength of Hoogsteen and Watson−Crick base pairing, respectively. It has been postulated that Watson−Crick base pairs are stronger that Hoogsteen base pairs (*21*); therefore, the presence of dU's in the Crick strand will decrease the hydrogen bonding strength in the most stable part of the molecule, yielding more destabilization.

Thermodynamic Unfolding Profiles. Our DSC experiments indicate both triplexes unfold in monophasic non-two-state transitions. This is consistent with previous reports (*26*) and suggests the presence of coupled triplex → duplex and duplex → random coil transitions. The presence of coupled transitions has been observed before in intramolecular triplexes (*15*, *25*, *26*), and it has been suggested that this may be a consequence of a lower entropy cost in their formation, which does not compensate for the unfavorable enthalpy of removing the third strand (*15*). This explanation is consistent with the observation that longer intramolecular triplexes (*34*), exhibiting an increased entropy penalty, usually unfold in biphasic transitions. The thermodynamic profiles in Table 1 indicate that the destabilizing effect of the inclusion of deoxyuridines is enthalpy-driven, suggesting a decrease in the level of stacking interactions. This is consistent with previous reports (*32*) and illustrates the stabilizing effect of C5 methyl groups; however, the stabilizing effect of the thymidine methyl groups may arise from both electronic and hydrophobic contributions. The electron donor properties of this methyl group may alter the aromaticity of its pyrimidine base, while its interaction with neighboring atomic groups or solvent molecules may result in favorable van der Waals and/or hydrophobic interactions. It has been suggested that the presence of methyl groups in nucleotides primarily affects the molecular polarizability of the bases (*22*, *23*), while hydrophobic effects may not adequately explain the stabilizing effect of methyl groups because substitutions of a hydrogen atom with a methyl group in uridine and cytosine increase their water solubility (*33*). Moreover, the presence of continuous stretches of methyl groups does have a stabilizing effect (*22*). Indeed, substitution of six alternating uridines with thymidines in $d(A_{12})/d(U_{12})$ was shown to induce a $\Delta G°$ stabilization of 1 kcal/mol, while substitution of six consecutive uridines resulted in a stabilization of 1.7 kcal/mol (*22*). This effect is due to the larger interaction of the induced dipole−induced dipole interactions of two consecutive uridine replacements; however, the contribution of direct contact between methyl groups was not discarded (*22*). In addition, the increased solubility of methyl-dC and dT with respect to dC and dU does not imply that the methyl groups of these bases lose their hydrophobic interactions but

rather that their inductive effect on the aromatic ring is compensating for the increased hydrophobicity of these substitutions.

The enthalpy for the unfolding of AU_2T and ATU_2 decreases as the sodium concentration increases, yielding negative heat capacity with smaller magnitudes for AU_2T and ATU_2 (Table 1). Positive heat capacity effects have been reported in the unfolding of proteins (*34*) and recently in the unfolding of nucleic acids (*35*−*38*). The presence of heat capacity effects has been attributed to the exposure of nonpolar groups to the solvent and/or to changes in structural hydration between the folded and unfolded states (*34*). Thus, the negative heat capacity effects measured indirectly with these intramolecular triplexes indicate that the overall helical states of these triplexes are slightly more hydrophobic than their random coil state. Furthermore, the fact that the heat capacity effects of AU_2T and ATU_2 are weaker than those of ATT suggests that the removal of two methyl groups from each triplex destroys the compact association of the double chain of methyl groups in their major groove, thus lowering the relative degree of exposure of hydrophobic groups to the solvent. This is accompanied by a decrease in the level of structural hydration, which may contribute with an exothermic heat, yielding lower transition enthalpies and reducing the stability of the triplex.

Thermodynamic Release of Counterions. The release of counterions of ATU_2 and AU_2T is smaller than that of ATT, suggesting that the presence of dU bases decreases their overall charge density parameter. This is consistent with the decrease in the number of stacking interactions observed in the DSC experiments, which will result in an increased distance between the negatively charged phosphates with a concomitant decrease in charge density. This effect probably reflects the difference in sodium concentration between the DNA surface and the solution. As the sodium concentration increases, the sodium gradient between the local environment of the DNA and the bulk solution decreases, resulting in a decrease in Δn_{Na^+} due to an increase in the level of counterion screening at higher salt concentrations. This effect is consistent with previous theoretical studies that showed an increase in the actual rate of release of counterions as the solution concentration of cations decreases (*39*). In addition, the rate of release of counterions decreases (ATT and ATU_2), and then it increases (AU_2T) as the concentration of salt increases, suggesting that ATT and ATU_2 form similar triplexes and consistent with the stability of ATU_2 being higher than that of AU_2T. Moreover, as the salt concentration increases, the stability of AU_2T approaches that of ATU_2, suggesting that AU_2T rearranges itself into a more stable triplex, perhaps approaching the structural features of ATU_2; i.e., the Δn_{Na^+} values of AU_2T gradually approach those of ATU_2, suggesting that their charge densities and structural features become more similar. At very high sodium concentrations, however, AU_2T appears to form a triplex structure with a much higher charge density. The overall trend indicates that although the structures of these triplexes may be very similar, there may be slight differences in their charge density distribution, which are reflected in their Δn_{Na^+} and heat capacity parameters; i.e., condensed ions and immobilized water are intimately connected in the formation of a particular DNA structure.

Interaction of Netropsin with Triplexes. In this study, netropsin is used as a probe of the grooves of these triplexes. Rentzeperis and Marky initially suggested the binding of a second netropsin molecule to the hydrophobic groove, formed by the double chain of the deoxythymidine methyl groups (*25*). Alternatively, the second netropsin could be binding to the cytosine loops or to the minor groove in a side-by-side fashion. The formation of these alternative complexes was discarded in their investigation (*25*) by showing that a control double-hairpin duplex with identical loops and similar minor groove could bind only one netropsin molecule. It is possible to argue that the minor groove of these triplexes may be different and may accommodate two netropsin molecules in a side-by-side fashion. This possibility seems unlikely due to the presence of a positive charge at each end of netropsin, which creates an electrostatic repulsion that prevents the formation of a side-by-side complex. In support of this hypothesis, the monocation distamycin, which forms a side-by-side complex in the minor groove, can accommodate three ligand molecules in the ATT triplex, two in the minor groove and one in the hydrophobic groove (*26*). The UV melts of the netropsin−AU_2T and netropsin−ATU_2 complexes result in biphasic transitions. The first transition corresponds to the triplex → duplex transition and is accompanied by the dissociation of the first netropsin, while the second transition corresponds to the duplex → coil transition and dissociation of the second netropsin. This indicates that the presence of netropsin stabilizes the duplex but destabilizes the triplex transition, consistent with previous literature reports (*25*, *26*, *40*), which show that netropsin destabilizes the association of the third strand. Our melting curves indicate that full formation of each netropsin−triplex complex can be guaranteed only at <8 °C (Figure 3c). Netropsin binds to AU_2T and ATU_2 (Table 2) with binding affinities of 10^4−10^7, exothermic heats, and multiple-site binding stoichiometries. Binding of netropsin to the first site (minor groove) is characterized by a higher affinity and slightly more exothermic heats than binding of netropsin to the first site of ATT. The destabilization due to the presence of dU bases in the stem of these triplexes might decrease the affinity of the third strand for the purine bases of the duplex. Therefore, the minor groove of these two triplexes will have characteristics which are closer to those of the minor groove of a DNA duplex with a $dA_7{\cdot}dT_7$ sequence than to those of the minor groove of ATT because similar binding profiles are obtained for binding of netropsin to the control duplex, $d(A_4C_5T_7C_5A_3)$, of previous investigations (*25*, *26*). On the other hand, binding of netropsin to the second site of these triplexes results in lower binding affinities and lower exothermic heats than binding to the corresponding site of ATT. These results are consistent with the lower affinity of the third strand for its duplex part, which yielded triplexes with lower stability. The weaker association of the third strand may be the result of a disrupted hydrophobic groove that interacts weakly with netropsin. Furthermore, the second site of ATU_2 and AU_2T binds an additional netropsin. This indicates that the presence of uridine yields triplexes that are more flexible or less compact than ATT, which contains an extended second binding site for netropsin. This effect is consistent with their decrease in the number of stacking interactions and charge density parameter. Moreover, the presence of deoxyuridines in the

center of this groove may result in the formation of two identical domains in the major groove of these triplexes, each of which spans more than three to four base triplets and binds one netropsin molecule. The binding stoichiometries of 2:1 netropsin−triplex complexes from CD titrations confirm the multiple-site binding stoichiometries. Additionally, the change in ellipticity upon binding of the second netropsin is much smaller than the change observed upon binding of the first netropsin, consistent with the presence of two distinct binding sites characterized by different environments. This type of discrepancy in the number of binding sites obtained from spectroscopic and ITC titrations has been observed previously (*41*, *42*) and has been attributed to the lower magnitude of the optical changes upon binding to secondary sites with lower binding affinities. This explanation is especially true in this case, where the changes in ellipticity of binding of netropsin to the second site are much smaller than the changes in ellipticity that accompanied binding to the first site. The CD results can only confirm the presence of two different types of binding sites in these triplexes.

Binding of netropsin to the first site of these triplexes yields lower exothermic enthalpies than its binding to the second site (Table 2). The magnitudes of these heats are consistent with our current picture regarding the heats of binding of minor groove ligands to dA·dT sequences; that is, deep netropsin penetration, and netropsin snugly fit in the minor groove of B-DNA, yields high exothermic heats with alternating sequences and very low heats with homosequences (*31*). The higher hydration level of homosequences explains this large heat difference because an additional endothermic contribution is taken into account for the removal of electrostricted water molecules from the minor groove of homosequences (*31*). The side-by-side binding of two distamycin molecules in the minor groove of DNA yields a larger exothermic enthalpy (*29*) than the binding of a single distamycin molecule because of the tighter placement of the ligands in this groove. In addition, relative to DNA synthetic polymers, lower exothermic heats are obtained with oligonucleotide duplexes. Binding of netropsin to the ATU_2 and AU_2T triplexes, relative to ATT, is more exothermic than binding to the minor groove and less exothermic than binding to the second site (double chain of methyl groups or the hydrophobic groove). This shows that the interaction of netropsin with the minor groove of AU_2T and ATU_2 reflects the slightly lower level of hydration of their minor groove (*31*) and emphasizes the hydrophobic role of the thymidine methyl groups in the binding of ligands to DNA. Moreover, the fact that netropsin senses the hydrophobic groove of these triplexes, through van der Waals interactions, suggests that these folded triplexes may interact somewhat more strongly with hydrophobic surfaces. In support of this idea, hydration experiments have shown that binding of the third strand to a duplex is accompanied by an uptake of structural (or hydrophobic) water, which is immobilized around hydrophobic groups (*43*).

CONCLUSIONS

We used a combination of optical and calorimetric techniques to study the thermodynamic consequences of incorporating dT → dU substitutions into intramolecular triplexes. Our results show that these substitutions result in the destabilization of triplexes, the degree of which increases as the number of uridine bases increases. This suggests that the presence of methyl groups plays an important role in the stabilization of triple helices. The inclusion of just two of these substitutions around the middle of seven TAT base triplets results in a decrease in the level of stacking interactions, charge density, and heat capacity effects. This suggests that methyl groups affect both the molecular polarizability of the base to which they are attached and the extent of hydrophobic interactions between neighboring atomic groups and solvent molecules. In addition, netropsin binding indicated that the presence of uridine bases disrupts the hydrophobic groove, lowering its cooperativity and resulting in the formation of two hydrophobic domains with decreased binding affinity. Our combined results indicate that the stabilizing effect of hydrophobic groups may arise from the combination of hydrophobic and electronic effects. One biological implication of these results relates to the recognition of H-DNA by triplex-binding proteins. The presence of a hydrophobic groove may be one of the distinctive features that allow the recognition of H-DNA by these proteins and may prove to be important in the modulation of the functions attributed to H-DNA. Furthermore, the presence of a stabilizing hydrophobic groove may help in the design of triplex-stabilizing ligands and nucleotide analogues that may eventually help in the development of triplexes as therapeutic agents. Moreover, the negative heat capacity effects measured indirectly with these triplexes suggest that the overall helical states of these triplexes may be slightly more hydrophobic than their duplex counterparts. This may present some advantages in the delivery of these molecules for therapeutic purposes.

REFERENCES

1. Bloomfield, V. A., Crothers, D. M., and Tinoco, I. (2000) *Nucleic Acids: Structure, Properties and Functions*, University Science Books, Sausalito, CA.
2. Thuong, N. T., and Helene, C. (1993) Sequence-Specific Recognition and Modification of Double-Helical DNA by Oligonucleotides, *Angew. Chem., Int. Ed. 32*, 666−690.
3. Helene, C. (1990) Rational Design of Sequence-Specific Oncogene Inhibitors Based on Antisense and Antigene Oligonucleotides, *Eur. J. Cancer 27*, 1466−1471.
4. Helene, C. (1994) Control of Oncogene Expression by Antisense Nucleic Acids, *Eur. J. Cancer 30A*, 1721−1726.
5. Dove, A. (2002) Antisense and Sensibility, *Nat. Biotechnol. 20*, 121−124.
6. Duval-Valentin, G., Thuong, N. T., and Helene, C. (1992) Specific Inhibition of Transcription by Triple Helix-Forming Oligonucleotides, *Proc. Natl. Acad. Sci. U.S.A. 89*, 504−508.
7. Maher, L. J., III, Wold, B., and Dervan, P. B. (1989) Inhibition of DNA Binding Proteins by Oligonucleotide-Directed Triple Helix Formation, *Science 245*, 725−730.
8. Soyfer, V. N., and Potaman, V. N. (1996) *Triple-Helical Nucleic Acids*, Springer-Verlag, New York.
9. Rajagopal, P., and Feigon, J. (1989) Triple-Strand Formation in the Homopurine:Homopyrimidine DNA Oligonucleotides d(G-A)$_4$ and d(T-C)$_4$, *Nature 339*, 637−640.
10. Beal, P. A., and Dervan, P. B. (1991) Second Structural Motif for Recognition of DNA by Oligonucleotide-Directed Triple-Helix Formation, *Science 251*, 1360−1363.
11. Moser, H. E., and Dervan, P. B. (1987) Sequence-Specific Cleavage of Double Helical DNA by Triple Helix Formation, *Science 238*, 645−650.
12. Lacroix, L., Lacoste, J., Reddoch, J. F., Mergny, J.-L., Levy, D. D., Seidman, M. M., Matteucci, M. D., and Glazer, P. M. (1999) Triplex Formation by Oligonucleotides Containing 5-(1-Propynyl)-2′-deoxyuridine: Decreased Magnesium Dependence and Improved Intracellular Gene Targeting, *Biochemistry 38*, 1893−1901.

13. Sugimoto, N., Wu, P., Hara, H., and Kawamoto, Y. (2001) pH and Cation Effects on the Properties of Parallel Pyrimidine Motif DNA Triplexes, *Biochemistry 40*, 9396−9405.
14. Plum, G. E., and Breslauer, K. J. (1995) Thermodynamics of an Intramolecular DNA Triple Helix: A Calorimetric and Spectroscopic Study of the pH and Salt Dependence of Thermally Induced Structural Transitions, *J. Mol. Biol. 248*, 679−695.
15. Soto, A. M., Loo, J. A., and Marky, L. A. (2002) Energetic Contributions for the Formation of TAT/TAT, TAT/CGC+, and CGC+/CGC+ Base-Triplet Stacks, *J. Am. Chem. Soc. 124*, 14355−14363.
16. Povsic, T. J., and Dervan, P. B. (1989) Triple Helix Formation by Oligonucleotides on DNA Extended to the Physiological pH Range, *J. Am. Chem. Soc. 111*, 3059−3061.
17. Völker, J., and Klump, H. H. (1994) Electrostatic effects in DNA triple helices, *Biochemistry 33*, 13502−13508.
18. Barszcz, D., and Shugar, D. (1968) Complexes of Poly-Ribothymidylic Acid with Poly-Adenylic Acids and Some Properties of Poly-Deoxyriboadenylic Acid, *Eur. J. Biochem. 5*, 91−100.
19. Escude, C., Francois, J.-C., Sun, J.-S., Ott, G., Sprinzl, M., Garestier, T., and Helene, C. (1993) Stability of Triple Helices Containing RNA and DNA Strands: Experimental and Molecular Modeling Studies, *Nucleic Acids Res. 21*, 5547−5553.
20. Lee, J. S., Woodsworth, M. L., Latimer, L. J. P., and Morgan, A. R. (1984) Poly(pyrimidine)·Poly(purine) Synthetic DNAs Containing 5-Methylcytosine form Stable Triplexes at Neutral pH, *Nucleic Acids Res. 12*, 6603−6614.
21. Leitner, D., Schroder, W., and Weisz, K. (2000) Influence of Sequence-Dependent Cytosine Protonation and Methylation of DNA Triplex Stability, *Biochemistry 39*, 5886−5892.
22. Wang, S., and Kool, E. T. (1995) Origins of the Large Differences in Stability of DNA and RNA Helices: C-5 Methyl and 2′-Hydroxyl Effects, *Biochemistry 34*, 4125−4132.
23. Wang, S., Xu, Y., and Kool, E. T. (1997) Recognition of RNA Triplex Formation: Divergent Effects of Pyrimidine C-5 Methylation, *Bioorg. Med. Chem. 5*, 1043−1050.
24. Xodo, L. E., Manzini, G., Quadrifoglio, F., van der Marel, G. A., and van Boom, J. H. (1991) Effect of 5-Methylcytosine on the Stability of Triple-Stranded DNA: A Thermodynamic Study, *Nucleic Acids Res. 19*, 5625−5631.
25. Rentzeperis, D., and Marky, L. A. (1995) Ligand Binding to the Hoogsteen-WC Groove of TAT Base Triplets. Thermodynamic Contribution of the Thymine Methyl Groups, *J. Am. Chem. Soc. 117*, 5423−5424.
26. Rentzeperis, D. (1994) Thermodynamics and Ligand Interactions of DNA Hairpins, Doctoral Dissertation, New York University, New York.
27. Cantor, C. R., Warshaw, M. M., and Shapiro, H. (1970) Oligonucleotide Interactions. III. Circular Dichroism Studies of the Conformation of Deoxyoligonucleotides, *Biopolymers 9*, 1059−1077.
28. Marky, L. A., Blumenfeld, K. S., Kozlowski, S., and Breslauer, K. J. (1983) Salt-Dependent Conformational Transitions in the Self-Complementary Deoxydodecanucleotide d(CGCGAATTCGCG): Evidence for Hairpin Formation, *Biopolymers 22*, 1247−1257.
29. Rentzeperis, D., Marky, L., Dwyer, T. J., Geierstanger, B. H., Pelton, J. G., and Wemmer, D. E. (1995) Interaction of Minor Groove Ligands to an AAATT/AATTT Site: Correlation of Thermodynamic Characterization and Solution Structure, *Biochemistry 34*, 2937−2945.
30. Marky, L. A., and Breslauer, K. J. (1987) Calculating Thermodynamic Data for Transitions of any Molecularity from Equilibrium Melting Curves, *Biopolymers 26*, 1601−1620.
31. Marky, L. A., and Kupke, D. W. (1989) Probing the Hydration of the Minor Groove of A·T Synthetic DNA Polymers by Volume and Heat Changes, *Biochemistry 28*, 9982−9988.
32. Soto, A. M., Gmeiner, W. H., and Marky, L. A. (2002) Energetic and Conformational Contributions to the Stability of Okazaki Fragments, *Biochemistry 41*, 6842−6849.
33. Sowers, L. C., Shaw, B. R., and Sedwick, W. D. (1987) Base Stacking and Molecular Polarizability Effect of a Methyl Group in the 5-Position of Pyrimidines, *Biochem. Biophys. Res. Commun. 148*, 790−794.
34. Makhatadze, G. I., and Privalov, P. L. (1990) Heat Capacity of Proteins. I. Partial Molar Heat Capacity of Individual Amino Acid Residues in Aqueous Solution: Hydration Effect, *J. Mol. Biol. 213*, 375−384.
35. Holbrook, J. A., Capp, M. W., Saecker, R. M., and Record, M. T., Jr. (1999) Enthalpy and Heat Capacity Changes for Formation of an Oligomeric DNA Duplex: Interpretation in Terms of Coupled Processes of Formation and Association of Single-Stranded Helices, *Biochemistry 38*, 8409−8422.
36. Chalikian, T. V., Völker, J., Plum, G. E., and Breslauer, K. J. (1999) A More Unified Picture for the Thermodynamics of Nucleic Acid Duplex Melting: A Characterization by Calorimetric and Volumetric Techniques, *Proc. Natl. Acad. Sci. U.S.A. 96*, 7853−7858.
37. Rouzina, I., and Bloomfield, V. A. (1999) Heat Capacity Effects on the Melting of DNA. 1. General Aspects, *Biophys. J. 77*, 3242−3251.
38. Rouzina, I., and Bloomfield, V. A. (1999) Heat Capacity Effects on the Melting of DNA. 2. Analysis of Nearest-Neighbor Base Pair Effects, *Biophys. J. 77*, 3252−3255.
39. Gueron, M., and Weisbuch, G. (1980) Polyelectrolyte Theory. I. Counterion Accumulation, Site-Binding, and Their Insensitivity to Polyelectrolyte Shape in Solutions Containing Finite Salt Concentrations, *Biopolymers 19*, 353−382.
40. Durand, M., Thuong, N. T., and Maurizot, J. C. (1992) Binding of netropsin to a DNA triple helix, *J. Biol. Chem. 267*, 24394−24399.
41. Rentzeperis, D., Alessi, K., and Marky, L. A. (1993) Thermodynamics of DNA Hairpins: Contribution of Loop Size to Hairpin Stability and Ethidium Binding, *Nucleic Acids Res. 21*, 2638−2689.
42. Rentzeperis, D., Medero, M., and Marky, L. A. (1995) Thermodynamic Investigation of the Association of Ethidium, Propidium and Bis-ethidium to DNA Hairpins, *Bioorg. Med. Chem. 3*, 751−759.
43. Rentzeperis, D., Tran, H., and Marky, L. A. (1994) Calorimetric Investigation of the DNA Triple Helix: d(CCT_5CCT_5CC)/d(GGA_5GA_5GG)/d(CCT_5CCT_5CC), *Biophys. J. 66*, A158.

BI052203B